The radiologic prediction of Alzheimer disease: the atrophic hippocampal formation.

M J de Leon, J Golomb, A E George, A Convit, C Y Tarshish, T McRae, S De Santi, G Smith, S H Ferris and M Noz

AJNR Am J Neuroradiol 1993, 14 (4) 897-906
http://www.ajnr.org/content/14/4/897

The Radiologic Prediction of Alzheimer Disease: the Atrophic Hippocampal Formation

M. J. de Leon,[1] J. Golomb,[2] A. E. George,[3] A. Convit,[1] C. Y. Tarshish,[1] T. McRae,[4] S. De Santi,[1] G. Smith,[1] S. H. Ferris,[1] M. Noz,[3] and H. Rusinek [3]

PURPOSE: To test the hypothesis that atrophy of the hippocampal formation in nondemented elderly individuals would predict subsequent Alzheimer disease. **METHOD:** We studied 86 subjects at two time points, 4 years apart. At baseline all study subjects were nondemented and included 54 control subjects and 32 persons who had memory complaints and minimal cognitive impairments. All subjects received a CT scan using a protocol designed to image the perihippocampal cerebrospinal fluid (HCSF) accumulating in the fissures along the axis of the hippocampal formation. Blind to the clinical evaluations, we subjectively assessed the presence of HCSF at the baseline. Retrospectively, we examined the predicted association between baseline HCSF and clinical decline as determined across the two evaluations. **RESULTS:** At follow-up 25 of the 86 subjects had deteriorated and received the diagnosis of Alzheimer disease. Of the declining subjects, 23 came from the minimally impaired group, and 2 came from the control group. In the minimally impaired group the baseline HCSF measure had a sensitivity of 91% and a specificity of 89% as a predictor of decline. Both control subjects who deteriorated were also correctly identified at baseline. One of these two subjects died, and an autopsy confirmed the presence of Alzheimer disease. Mr validation studies demonstrated that HCSF is quantitatively related to dilatation of the transverse fissure of Bichat and the choroidal and hippocampal fissures. **CONCLUSION:** Our findings strongly suggest that among persons with mild memory impairments, dilatation of the perihippocampal fissures is a useful radiologic marker for identifying the early features of Alzheimer disease.

Index terms: Dementia; Degenerative brain disease; Hippocampus; Brain, atrophy; Brain, computed tomography; Brain, magnetic resonance; Age and aging; Memory

AJNR 14:897–906, July/August 1993

Current knowledge, derived across species from cross-sectional studies, suggests that damage to the hippocampus is at least in part related to age-related decline in memory functioning (1–3). In normal human aging, Alzheimer-type histopathologic findings limited to the hippocampus are commonly observed. The 7th to 10th decades of normal human aging show consistent vulnerability for hippocampal neuronal loss, neurofibrillary tangles, granulovacuolar degeneration, and senile plaques (4–7).

In Alzheimer disease (AD), which typically involves widespread neuropathology, the above-mentioned age-associated histpathololgic changes are markedly exacerbated in the hippocampus. The observations of hippocampal pathology across the continuum of normal aging to AD have led researchers to examine the hippocampus and its intimately connected parahippocampal gyrus as potential sites for the earliest neurodegenerative changes associated with AD (8). Comparing nondemented elderly with and without neuropathologic evidence of AD, de la Monte (9) found that hippocampal volume reductions were associated with positive histologic findings. Another group reported that patients with very mild dementia often showed neurofibrillary tangles in the hippocampal region (7, 10). In more

Received October 20, 1992; revision requested December 18 and accepted March 18, 1993.

This work was in part funded by USPHS Grants NIA P30 AG08051, P50 MH43486, and RO1 MH43965, and by the Orentreich Foundation for the Advancement of Science and Mrs. Betty Wold Johnson.

Departments of [1] Psychiatry, [2] Neurology, [3] Radiology, and [4] Medicine, New York University Medical Center, 550 First Ave, New York, NY 10016. Address reprint requests to Dr. Mony J. de Leon.

AJNR 14:897–906, July/August 1993 0195-6108/93/1404–0897

advanced AD cases, tangles were found throughout the neocortex. These cross-sectional studies point to the hippocampus and related structures as potentially very early sites of involvement in AD.

The in vivo neuroimaging of the hippocampus has only recently been considered possible. Consequently, very limited data exist for normal aging and AD. Several magnetic resonance (MR) studies of clinically probable AD have reported parenchymal volume losses in the hippocampus and parahippocampal gyrus (11–13). One computed tomography (CT) study reported that neuropathologically confirmed AD cases, studied within a few years of death and suffering with severe dementia, showed reduced hippocampal size (14).

CT and MR studies by de Leon and colleagues examined cerebrospinal fluid accumulation in the fissures of the perihippocampal region (HCSF) in both normal aging and AD (15–17). These studies used a negative-angulation axial scan plane, which enabled imaging of the long axis of the hippocampal region and subjective assessment of the HCSF. In a cross-sectional CT study of 175 patients with AD and healthy elderly control subjects, this group reported a very high prevalence of HCSF (>80%) in memory-impaired individuals (16). The results indicated that HCSF, despite increasing in prevalence with age among control subjects, was useful for supporting the clinical diagnosis of AD. Most importantly, longitudinal results (n = 41) from this study indicated that HCSF predicted the development of dementia among individuals with mild cognitive impairments that were insufficient to warrant a diagnosis of AD.

Previous neuroanatomic work has identified at least three major perihippocampal fissures that may contribute to the appearance of HCSF. These fissures include the lateral part of the transverse fissure of Bichat (TFB), the choroidal fissure, and the hippocampal fissure (18). Neuropathologic and postmortem MR imaging studies in AD by de Leon and colleagues have revealed that dilatation of these fissures reflects parenchymal volume loss from the hippocampus and the parahippocampal gyrus. Adjacent thalamic and midbrain structures do not typically show sufficient neuropathologically determined volume reductions in AD to account for the HCSF findings (17, 19, 20).

The longitudinal normal aging CT study reported here firmly establishes that, in elderly patients with minimal cognitive impairments, HCSF accurately predicts the development of dementia consistent with the clinical diagnosis of AD.

Subjects and Methods

All subjects signed informed consent in order to participate in the study. These subjects were either recruited as volunteer control subjects or were referred to our Alzheimer disease center clinic for evaluation of memory and other cognitive complaints. All elderly subjects seen between 1984 and 1991 who completed baseline and 4-year follow-up evaluations and who met screening criteria (see below) were included in a longitudinal study cohort. For this study we retrospectively selected from the cohort only the 86 nondemented subjects. (See below for the distinction between demented and nondemented status.)

The baseline and follow-up examinations consisted of medical, neurologic, psychiatric, neuropsychologic, and neuroradiologic examinations. In order to obtain a pure sample of study subjects, persons with diseases that could affect brain functioning were excluded. Conditions that warranted exclusion were any history or neurologic evidence of stroke, CT evidence of infarction, a Hachinski ischemia rating scale score greater than 3 (21), or significant psychiatric, cardiac, endocrinologic, hematologic, hypertensive, gastrointestinal, pulmonary, immunologic, metabolic, or neoplastic diseases. Hence, a medically healthy group of elderly subjects was selected and longitudinally followed.

Psychiatric and Neuropsychologic Measures

As part of the clinical examination, all subjects received ratings on the Global Deterioration Scale (GDS) (22) and an independently administered formal psychometric evaluation. Previous studies using the GDS have demonstrated excellent interrater reliability (23, 24) and good correlations with other dementia rating scales (25). The GDS evaluates the general level of functioning and is rated on a seven-point scale using specific clinical anchor points. Increasing scale values indicate increased functional impairment. For those subjects showing deficits, family members were interviewed concerning the patient's ability to perform tasks of daily living.

High-functioning healthy elderly persons do not show any clinically verifiable deficits and receive GDS scores of 1 or 2 depending on whether they have self-reported memory complaints. Minimally impaired subjects, those with GDS scores of 3, typically show mild memory impairments and/or mild word- and name-finding deficits, present with complaints of mild cognitive decline that are verified by family members, but remain competent in activities of daily living. Dementia patients show deficits in multiple cognitive areas of sufficient magnitude to impair day-to-day functioning and therefore have GDS scores of 4 or greater. The criteria for a GDS of 4 agree with those established by the DSM III-R (26) and NINCDS-ADRDA criteria (27) as defining AD.

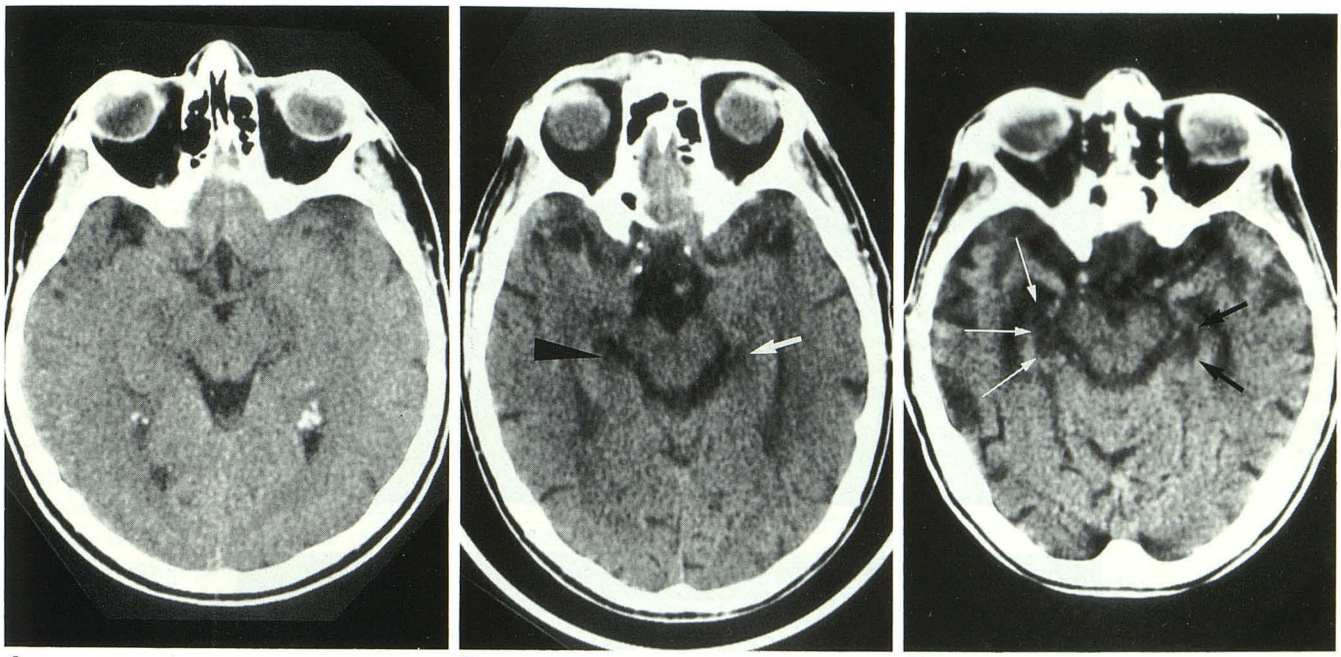

Fig. 1. Negative-angulation axial CT views depicting three examples of the HCSF ratings.
A, A 64-year-old woman (GDS = 2) with a bilaterally normal scan (HCSF = 0).
B, A study from an 80-year-old man (GDS = 3) shows mild hippocampal atrophic changes in the right hemisphere (HCSF = 2, *large black arrowhead*) and questionable atrophy (HCSF = 1, *white arrow*) in the left.
C, A 55-year-old woman (GDS = 3) shows severe right hippocampal atrophy (HCSF = 3, *three white arrows*) and moderate atrophy on the left (HCSF = 2, *two black arrows*).

At baseline, study subjects ranged from highly functional control subjects to persons with minimal impairment. This study group was composed of 54 subjects with GDS of 1 to 2 and mean age 70.1 ± 8.0 (±SD) and 32 subjects with GDS of 3 and mean age 71.1 ± 9.4. The groups with GDS of 1 or 2 and GDS of 3 had comparable follow-up intervals of 3.7 ± 1.1 and 4.1 ± 1.5 years, respectively ($t(84) = 1.3$, $P > .05$). By follow-up, 25 of the subjects received a GDS rating of at least 4 and had developed symptoms of AD fulfilling DSM III-R and NINCDS-ADRDA criteria.

In order to examine cognitive performance as a predictor of decline, all subjects received a psychometric test battery derived from the Guild Memory Test (28) and the Wechsler Adult Intelligence Scale (29). The battery included the immediate and delayed recall of two paragraphs, immediate and delayed recall of 10 verbal paired associates, recognition recall of 10 abstract designs, a digit symbol substitution test, and digits forward and backward. To reduce the number of psychometric variables, we developed a composite psychometric score averaging the percent correct from each of the eight subtests.

Because this study began before our systematic inclusion of the Mini Mental Status Examination (MMSE) (30), not all the cases have this measure. For reference purposes the control subjects in this study had mean MMSE scores of 29 ± 2 (n = 47). The MMSE scores of the minimally impaired patients averaged 25 ± 4 (n = 25), which was significantly lower than control ($t(70) = 5.4$, $P < .001$).

HCSF Evaluations

Anatomic Studies. At baseline, CT scans were obtained with either a GE 8800 or GE 9800 scanner and at follow-up with the GE 9800 scanner (General Electric, Milwaukee, WI). All subjects were studied using two protocols, one for the HCSF evaluation and one for cortical and ventricular evaluations. The HCSF scan protocol included six contiguous 5-mm-thick sections through the temporal lobes at an infraorbital-meatal angulation of 20° to 25° negative to the canthomeatal plane. This so-called negative-angulation plane, in the region of the hippocampus, runs approximately parallel to the plane of the TFB, hippocampus, and temporal horn of the lateral ventricle. The negative-angulation CT scan permits a good view of the anterior-posterior extent of the perihippocampal region. With a 5-mm-thick section this region can be examined on two or three sections. When dilated the perihippocampal fissures appear on the negative-angulation scan as a pool of CSF medial to the hippocampal body (see Fig. 1). This CSF pool is what we call HCSF.

In order to demonstrate visually the anatomic source of the CSF contributing to the evaluation of HCSF, we selected a moderately atrophic patient with AD and using a General Electric Advantage (Waukesha, WI) 1.5-T imager obtained a T1-weighted gradient-echo coronal MR study with a 1.3-mm section thickness. We drew perihippocampal fissure regions of interest (ROIs) on 56 coronal images

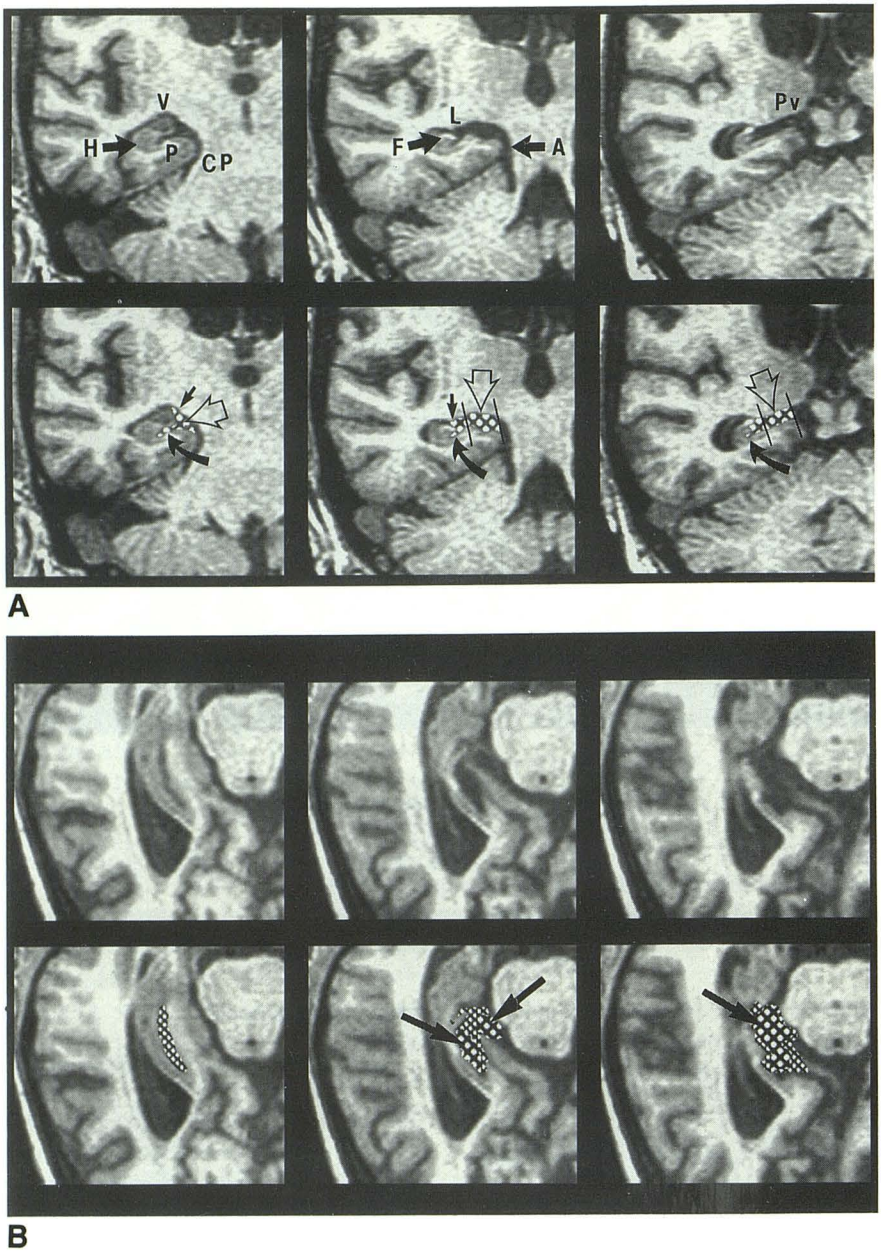

Fig. 2. The MR scans were obtained on a GE Advantage 1.5-T imager using a spoiled gradient-echo sequence of 35/9/1 (TR/TE/excitations), a 60° flip angle, an 18-cm field of view, and a 256 × 128 acquisition matrix. We obtained 124 contiguous coronal images with a section thickness of 1.3 mm. On 56 of these images, using a twofold image magnification (new pixel size = 0.35 mm) to aid in region drawing, we outlined a perihippocampal CSF region including the TFB, the choroidal fissure, and the hippocampal fissure. The image intensity values in this region were coded as *large open circles* (*A*). All 56 coronal images and the coded region were reformatted into a negative-angulation axial plane and transformed (by averaging) into 5-mm contiguous sections (*B*). The reformatted axial images in *B* show as *large open circles* the HCSF originally drawn on the coronal scan (*A*). The *small open circles* surrounding the *large open circles* represents the partially volumed pixels. The lateral boundary for the perihippocampal fissures was the choroid plexus of the temporal horn of the lateral ventricle and the hippocampus. If the choroid plexus was not visible, the middle of the fimbria was selected as an unbiased boundary between ventricle and the choroidal fissure. The medial boundary between the TFB and the blending ambient cistern was drawn as a line originating at the most medial and horizontal aspect of the subicular (superior) surface of the parahippocampal gyrus and extending dorsally to the inferior and horizontal aspect of the thalamus. Consequently, the linear medial boundary approximated a perpendicular between two parallel surfaces. Once the medial and lateral margins for the fissures were identified, an ROI was drawn around the area. A signal intensity threshold was used to determine the pixels in the ROI containing CSF. The threshold was determined, section by section, as the average intensity between pure gray matter and CSF based on eight gray matter samples taken from the frontotemporal cortical ribbon and eight CSF samples taken from the lateral ventricle.

A, Top row, V = Choroid plexus and temporal horn of lateral ventricle; H = hippocampus; P = parahippocampal gyrus; CP = cerebral peduncle; L = lateral geniculate body; F = fimbria; A = ambient cistern; Pv = pulvinar.

A, Bottom row, HCSF is coded as *large open circles.* Hippocampal fissure (*curved arrow*), choroid fissure (*small arrow*), TFB (*open arrow*). *Parallel lines* indicate locations for height measurement as defined in appendix.

B, Bottom row, Straight arrows indicate the pure CSF coded with the *large open circles.*

and examined the ROIs on a reformatted axial plane of section (see Fig. 2). The reformatted negative-angulation axial plane was imaged as contiguous 5-mm sections in order to approximate the conditions of the clinical study. The figure shows that the HCSF seen on the axial view is predominantly related to the CSF accumulating in the TFB and the related choroidal and hippocampal fissures. HCSF is not likely to be caused by CSF accumulations in the ambient cistern or the temporal horn of the lateral ventricle. In the Appendix we provide information on the quantitative anatomic validation of the HCSF observation.

Ratings of HCSF. Retrospectively and blind to patient clinical status, all baseline CT scans were rated for the magnitude of HCSF. As in our earlier work (15–17) we used a subjective four-point rating scale (0 = none, 1 = questionable, 2 = mild to moderate, and 3 = severe). A score of 2 or greater was considered evidence of HCSF (see Fig. 1A–1C). A case was classified as atrophic if at least one hemisphere showed HCSF. These dichotomous groupings have excellent reliability. Two observers independently rated 25 scans randomly selected from 146 study scans. The agreement between observers for HCSF was $\kappa = 0.92$ and 1.0 for the right and left hemispheres, respectively. There was 100% agreement for the identification of atrophic cases. In a separate study of HCSF we found an excellent correspondence between axial MR and CT ratings of the same patient (see Appendix, Study 1).

CT Evaluation of Generalized Atrophic Change. To compare the evaluations of HCSF with more conventional methods of clinical scan assessment, a second set of CT data was obtained. This protocol yielded 10-mm-thick contiguous sections from the base of the brain to the vertex in a conventional plane parallel to the canthomeatal plane. Using this second protocol we separately rated the overall extent of ventricular enlargement and sulcal prominence (cortical atrophy) using seven-point scales. This scale was derived from our previously published four-point scale, which included anchor reference cases for each of the points (31). In the present study we included three additional intermediate levels of observed atrophy between the four anchor points of 1 (normal), 3 (mild), 5 (moderate), and 7 (severe). The additional rating points were scored 2 for very mild, 4 for mild to moderate, and 6 for moderate to severe.

In addition, a quantitative measurement of linear ventricular size was made. Five anatomically defined linear measurements were made at midventricular levels from the one or two sections that best depicted the frontal horns of the lateral ventricle and the third ventricle at the level of the basal ganglia and foramen of Monro (32). The five linear measurements were each corrected for brain size using a colinear inner table to inner table skull measurement and averaged to provide an overall ventricle/brain ratio. Earlier work with the linear ventricular size estimate indicated that it is highly reliable across observers ($r = .91$, $P < .001$, $n = 109$), highly correlated with ventricular volumes in normal aging and AD and useful in describing longitudinal change (32).

Results

Over the study interval 25 of 86 subjects showed cognitive decline and met criteria for probable AD at follow-up. At baseline, 23 of the subjects who declined had been in the group with GDS of 3 (n = 32), resulting in a 72% decline frequency for this group. Only 2 (4%) of the group with GDS of 1 or 2 (n = 54) declined. Consequently, further statistical analyses were confined to the group with GDS of 3. This minimally impaired group presents an important clinical challenge in predicting who will deteriorate and receive a probable AD diagnosis. Within this group, the mean follow-up intervals for the declining and nondeclining patients were the same at 4.1 years ($t(30) = .02$, $P > .05$). Decliners and nondecliners were also equivalent in years of education. Both groups averaged 13 years.

Using discriminant function classification analyses, for each baseline measure we determined the statistical significance of the relationship between actual and predicted clinical outcome. From the 2 × 2 classifications tables derived from the discriminant function analysis, the predictors of decline were examined for their sensitivity (percent correct identification of decliners) and specificity (percent correct identification of nondecliners). An overall predictive accuracy was also calculated (see Eq [1]). The sensitivity, specificity, and overall accuracy results are summarized in Table 1.

$$\text{Overall accuracy} = \frac{\text{Correctly predicted (declining + nondeclining) cases}}{\text{total N of cases}} \quad [1].$$

Hippocampal Atrophy

Discriminant function analysis showed that the CT rating of HCSF at baseline accurately differ-

TABLE 1: Sensitivity, specificity, and overall accuracy for predictors of decline

Measure	Decliners (n = 23) Sensitivity (%)	Nondecliners (n = 9) Specificity (%)	Total (n = 32) Overall (%)
HCSF	91	89	91[a]
Age	65	78	69
Sex	68	23	50
Psychometrics	70	89	75[b]
Cortical rating	74	33	63
Ventricle rating	60	56	59
Ventricle measurement	74	78	75[b]

[a] $P < .01$; [b] $P < .05$ (based on discriminant function analysis).

entiated between individuals who declined and reached a diagnosis of AD and those who did not ($F(1,30) = 46.0$, $P < .001$). The overall accuracy of HCSF for the prediction of the outcome was 91%. The sensitivity and specificity of the measure were 91% and 89%, respectively (see Table 1).

The results indicate that the observation of unilateral HCSF is sufficient to predict decline. Among the 21 decliners with HCSF in the group with GDS of 3, 9 had unilateral HCSF (5 left and 4 right hemisphere) and 12 bilateral. Similar prediction accuracies were found for the unilateral and bilateral subgroups ($\chi^2(1) = 1.3$, $P > .05$). The accuracy of prediction of decline was 90% for the unilateral and 100% for the bilateral group.

In order to assess further the prediction accuracy obtained for the hippocampal assessment, HCSF was compared with other potential predictors of decline, namely age, gender, psychometric test performance, and effects of generalized brain atrophy. These findings are summarized in Table 1 above.

Age. Age was not useful for the prediction of decline ($P > .05$). The average ages for the decliners and the nondecliners were not statistically different, 69 ± 9 and 75 ± 9 years, respectively ($t(30) = 1.6$, $P > .05$). The overall accuracy of age for the prediction of decline was very low.

Gender. Gender was not useful for predicting decline ($P > .05$). Decline was observed in 68% of the men and 77% of the women. The 13 men who declined were not significantly different in age from the 10 women who declined ($t(21) = 1.7$, $P > .05$).

Psychometric Test Performance. Lower baseline psychometric performance significantly predicted decline ($F(1,30) = 10.9$, $P < .01$) but had only modest overall prediction accuracy (75%). Sensitivity for predicting decline was weak (70%), but the psychometric evaluation showed good specificity (89%).

Generalized Brain Atrophy. We evaluated the cortical atrophy rating, the ventricular size rating, and the linear estimate of ventricular size as predictors. Only the linear measurement of ventricular enlargement showed a significant predictive relationship with decline ($F(1,30) = 7.2$, $P < .05$). The linear ventricular size measure achieved only a modest overall prediction accuracy score of 75%.

Finally, in order to explore the possibly unique value of HCSF to predict cognitive decline, direct comparisons were made between HCSF and the two other measures that reached significance as predictors. Multiple regression analyses showed that the psychometric measure when used alone accounted for 27% of the variance in the prediction of decline. The addition of HCSF significantly increased the explained variance by 39%, ($F_{change} = 32.7$, $P < .0001$). Similarly, the 19% of variance explained by the linear ventricle measure alone was increased by 41% with HCSF added, ($F_{change} = 31.0$, $P < .0001$). However, HCSF alone accounted for 61% of variance, which was improved by less than 5% with the inclusion of either the psychometric or the linear ventricle measures. These results demonstrate that HCSF was the superior predictor of decline.

Discussion

This study indicates that in the presence of minimal cognitive impairment, HCSF (dilatation of the perihippocampal fissure complex) is highly predictive of progressive deterioration and the clinical diagnosis of AD. Our validation studies demonstrate that dilatation of the perihippocampal fissures, particularly the TFB, accounts for the observation of HCSF (see Fig. 2 and Appendix, Study 2). The enlargement of the perihippocampal CSF spaces is likely caused by hippocampal formation atrophy (19–20a), and HCSF is easily determined with routine CT or MR equipment in a clinical setting. In comparison with other clinical and CT measures, HCSF was the superior predictor of decline to AD, and when combined with other baseline measures it greatly enhanced the overall predictive accuracy.

Other studies have found that psychological tests are predictive of future cognitive decline in cases of mild AD and of minimally impaired elderly (33, 34). The present study adds an anatomic predictor that adds to the predictive ability of a psychological test battery. The results from our study highlight the importance of including hippocampal evaluations in the clinical examination of age-related memory disorders. The results also provide a method for predicting decline that is independent of the educational and socioeconomic factors that may limit the usefulness of assessments based on psychologic testing alone.

The general relationship between hippocampal integrity and memory functioning is well characterized (1–3). However, the temporal relationship and consequently the interaction between the hippocampal atrophy and the subsequent neocortical and general intellectual degeneration that

occurs with AD is not well understood. Although it has not been demonstrated directly that limbic changes precede neocortical changes, several neuropathology studies suggest hippocampal and parahippocampal abnormalities as relatively early and specific phenomena (7, 35–38). The present study indicates that at a gross radiologic level, HCSF is consistently detected in the scans of nondemented patients destined to develop dementia, but generalized cortical atrophy and ventricular dilatation are not consistently detected before the decline. Thus, these longitudinal in vivo results lend further support to the hypothesized early appearance of hippocampal atrophy before clinical dementia. This interpretation of our findings is bolstered by Morris et al (10) and Price et al (7), who found at postmortem that very mildly demented patients have concentrated damage in the hippocampus and meet neuropathologic criteria for the diagnosis of AD.

In the absence of an in vivo diagnostic test for AD, and in the absence of diagnostic specificity data for our findings, we are forced to suggest cautiously that medically healthy elderly persons with minimal cognitive impairments in association with HCSF represent an early stage of AD. To some extent, support for this reasoning comes from our longitudinal data. Most of our subjects had follow-up CT scans that were comparable to the baseline scan. We found nearly a twofold increase in the annual rate of change in linear ventricular size for 12 of the declining subjects with GDS of 3 compared with 44 nondeclining (GDS of 1 and 2) control subjects, 2% and 1%, respectively ($t(54) = 2.5$, $P < .05$). This result is comparable to the magnitude of longitudinal ventricular change reported by other studies of AD patients (32, 39–41). In addition, of the 8 subjects who participated in the longitudinal study and died, one (who at baseline was cognitively normal and had HCSF) came to autopsy 9 years after the baseline. At the time of death this severely demented 82-year-old man was found to meet neuropathologic criteria for AD.

Our very limited data suggest but do not permit us to conclude that HCSF also may be a risk factor among healthy elderly. We found that both of the control subjects who declined to dementia levels had HCSF at baseline. However, six control subjects with HCSF at baseline did not develop symptoms of AD. Related evidence supporting the risk factor concept comes from Golomb et al, who demonstrated in a cross-sectional design that among healthy elderly persons (GDS of 1 or 2 and MMSE score $\geq$ 28), those with HCSF perform more poorly on psychometric measures of delayed recall than those without HCSF (42). To evaluate how well HCSF predicts progressive neuropsychologic decline in normals and the relationship of these changes to the pathologic diagnosis of AD will require additional study subjects, quantitative measures of HCSF, longer observation intervals, sensitive neuropsychological evaluations, and neuropathologic studies.

The results from our validation study 1 (as summarized in the Appendix) show an excellent correspondence between CT and MR estimates of HCSF. Given these results, we recommend the routine clinical use of either the negative-angle CT or MR to examine the brain of elderly patients with cognitive impairment for evidence of excess HCSF. However, the present study was not designed to identify the optimal section thickness for maximizing the sensitivity and specificity of the HCSF assessment with respect to prediction of decline. The results from our validation studies suggest that axial section thicknesses ranging from 4 to 6 mm are equivalent for the detection of HCSF. Extending HCSF evaluations to very thin axial scans or to the coronal plane will potentially require refined definitions for the diagnosis of clinically meaningful HCSF.

In summary, the present study identifies a predictive anatomic marker for future symptoms of AD. This marker should be useful in the identification of other biologic markers and in the selection of subjects for early experimental treatment.

Appendix: MR Validation Studies of HCSF

We used the multiplanar imaging capabilities of MR to answer questions concerning the anatomic basis of HCSF. First we demonstrated, using axial plane images, that MR assessments of HCSF were on a hemisphere-by-hemisphere basis, equivalent to the CT assessments of HCSF used in the current clinical longitudinal study. Second, we demonstrated that direct measurements of transverse fissure height and volume on coronal scans were strongly associated with the HCSF ratings determined from the axial scan.

Study 1: Comparison of Axial CT and MR Assessments of HCSF

Introduction. In 1987 our AD center began the transition from CT to MR. During this period, in

order to assess the correspondence between the machines, 53 subjects were studied on both CT and MR machines within an interval of 3 ± 3 months.

Method. The 5-mm negative-angulation CT protocol was the same as described in the body of the paper. The comparison MR protocol used a Phillips (Einhoven, The Netherlands) Gyroscan 1.5-T imager and included T1-weighted images (630/20/1) (TR/TE/excitations) through the entire temporal lobe in a negative-angulation axial plane parallel to the long axis of the hippocampal body. In most cases, the MR study was more steeply (negatively) angulated than the CT study by an approximate difference of 15 degrees. The MR axial sections were either 5 mm (n = 27) or 6 mm (n = 26), both with 10% gaps. All studies were done retrospectively and blind to clinical status and to the ratings on the other machine.

Results. Independent evaluation of the hippocampal region for each machine was in agreement for the presence or absence of HCSF in 52 out of 53 cases. Of the 52 concordant cases, 21 were diagnosed as nonatrophic, and 31 were diagnosed with HCSF. The overall classification agreement was determined to be $\kappa = .96$, $P < .0001$. Comparing CT and MR machines hemisphere by hemisphere, we found no discrepancies using MR section thicknesses of 5 mm and four discrepancies at 6 mm. Three of the four hemispheric discrepancies involved a failure to detect HCSF on the 6-mm MR. As two of these discrepancies occurred in one case, this resulted in the one misclassified patient. No relationship was found between MR section thickness and the agreement between machines for the diagnosis of HCSF ($\chi^2 = 1.1$, $P > .05$).

Study 2: Validation of HCSF with CSF Measurements

Introduction. After study 1 established the strong comparability between the CT and the MR for the subjective detection of HCSF, we used the MR for the anatomic validation of HCSF. As the HCSF rating is subjective and influenced by the partial voluming of perihippocampal fissure CSF with adjoining parenchyma, we undertook to examine the relationship between HCSF and direct quantitative measurements of the fissures.

Method. Two independent measurements of the fissures were made on the coronal scans; one was the height of the TFB (dorsal-ventral dimension), and the second was the total volume of all three fissures. We studied a separate patient group that met the above patient selection criteria and was composed of 22 persons with GDS of 1 and 2 and 55 with GDS of at least 3. Using the same Phillips Gyroscan equipment as in validation study 1, we obtained 4-mm-thick coronal MR scans and either 4-mm (n = 35) or 6-mm (n = 42) thick axial scans, all acquired with a 10% gap and using a T1-weighted 630/20/1 spin-echo sequence. The plane of the MR negative-angulation axial study was as described above, and the coronal plane was acquired perpendicular to the axial plane.

Height was measured on each coronal slice (ranging from three to five slices) from just posterior to the head of the hippocampus through the body and tail of the hippocampus, ending in the posterior hippocampus at the level of the ascending fimbria and the splenium of the corpus callosum. From an image projected onto a screen at a constant magnification factor of 2.5 times life size, we measured a lateral and a medial linear distance (height) of the CSF space between the superior surface of the parahippocampal gyrus and the inferior aspect of the thalamus. For each height an effort was made to standardize the site of the measurement by using visible landmarks. The most medial and horizontal aspect of the subiculum of the parahippocampal gyrus and the cornu ammonis defined the respective medial and lateral boundaries (see Fig. 2). For the thalamus, the landmarks included the lateral geniculate or pulvinar depending on the anterior-posterior location of the slice. For each hemisphere the average height across slices was calculated.

The second measurement consisted of the volume of the CSF for the perihippocampal fissures. The volume measurements were made on 38 randomly selected individuals from the 77 study subjects on which the height measurements were made. Volumes were determined across the same anatomically defined range of coronal sections as the heights using the same anatomic boundaries described as part of Figure 2. A Sun Workstation (Mountainview, CA) and our proprietary software were used to draw the anatomic ROIs. Under conditions of 2-fold magnification to aid in the drawing of the fissures, a best-CSF pixel intensity threshold was determined by visual inspection of the filling of the CSF spaces. The volumes were calculated as the average volume across sections (number of pixels CSF **x** (FOV/Matrix)^2 **x** section thickness/number of sections = volume).

Results and Conclusion. For both height and volume as dependent variables, separate two-way analyses of variance were run. These analyses were performed for right and left hemispheres individually in order to examine the relationships between subjective assessments of HCSF, section thickness, and their interaction. For all possible comparisons, no interactions were found between section thickness and HCSF ($Fs < 3$, $P > .05$). The failure of the interaction terms to reach significance indicates that the axial section thickness selected (4 mm or 6 mm) did not grossly influence the determination of HCSF. Significant main effects ($Ps < .001$) were found between HCSF and both the height of the transverse fissure ($F_{right}(1,73) = 47$ and $F_{left}(1,73) = 30$) and the volume of the transverse fissure ($F_{right}(1,34) = 24$ and $F_{left}(1,34) = 14$).

The mean TFB heights and standard deviations for the hemispheres with negative HCSF ratings were 2.8 mm ± 0.9 for both right and left; the TFB heights of the hemispheres with positive HCSF ratings were 4.3 mm ± 1.0 and 4.1 mm ± 1.1 for the right and left hemispheres, respectively. This represents an average TFB height increase of approximately 50%. For the volumes, HCSF negative right and left hemisphere averaged 0.45 ± 0.21 cc and 0.55 ± 0.24 cc, respectively; the corresponding values for the HCSF positive right and left hemispheres were 0.95 ± 0.37 cc and 1.03 ± 0.44 cc, respectively. This represents an average CSF volume increase of 98% for HCSF-positive compared with HCSF-negative cases. Therefore, subjectively identified HCSF is associated with quantitatively determined enlarged fissure size.

Acknowledgments

We are grateful for the excellent advice given by Dr. Irvin Kricheff and Dr. L. A. Saint Louis. We are indebted to Ms. Martha Helmers, Mr. Anthony Jalandoni, and Ms. Elizabeth Orleman for their high standards of craftsmanship.

References

1. Zola-Morgan S, Squire LR, Amaral DG. Human amnesia and the medial temporal region: enduring memory impairment following a bilateral lesion limited to field CA1 of the hippocampus. *J Neurosci* 1986;6:2950–2967
2. Kadar T, Silbermann M, Brandeis R, Levy A. Age-related structural changes in the rat hippocampus: correlation with working memory deficiency. *Brain Res* 1992;512:113–120
3. Moscovitch M, Winocur G. The neuropsychology of memory and aging. In: Craik FIM, Salthouse TA, eds. *The handbook of aging and cognition*. Hillsdale, NJ: Lawrence Erlbaum Associates, 1992:315–372
4. Ball MJ. Topographic distribution of neurofibrillary tangles and granulovacuolar degeneration in hippocampal cortex of aging and demented patients. A quantitative study. *Neuropathologica* 1978; 42:73–80
5. Kemper T. Neuroanatomical and neuropathological changes in normal aging and in dementia. In: Albert ML, ed. *Clinical neurology of aging*. New York: Oxford University Press, 1984:9–52
6. Terry RD, Peck A, De Teresa R, Schechter K, Horoupian DS. Some morphometric aspects of the brain in senile dementia of the Alzheimer type. *Ann Neurol* 1981;10:184–192
7. Price JL, Davis PB, Morris JC, White DL. The distribution of tangles, plaques and related immunohistochemical markers in healthy aging and Alzheimer's disease. *Neurobiol Aging* 1991;12:295–312
8. Hyman BT, Van Hoesen GW, Damasio AR, Barnes CL. Alzheimer's disease: cell-specific pathology isolates the hippocampal formation. *Science* 1984;225:1168–1170
9. de la Monte SM. Quantitation of cerebral atrophy in preclinical and end-stage Alzheimer's disease. *Ann Neurol* 1989;25:450–459
10. Morris JC, McKeel DW, Storandt M, et al. Very mild Alzheimer's disease: informant-based clinical, psychometric, and pathological distinction from normal aging. *Neurology* 1991;41:469–478
11. Seab JP, Jagust WS, Wong SFS, Roos MS, Reed BR, Budinger TF. Quantitative NMR measurements of hippocampal atrophy in Alzheimer's disease. *Magn Reson* 1988;8:200–228
12. Kesslak JP, Nalcioglu O, Cotman CW. Quantification of magnetic resonance scans for hippocampal and parahippocampal atrophy in Alzheimer's disease. *Neurology* 1991;41:51–54
13. Jack CR Jr, Petersen RC, O'Brien PC, Tangalos EG. MR-Based hippocampal volumetry in the diagnosis of Alzheimer's disease. *Neurology* 1992;42:183–188
14. Jobst KA, Smith AD, Szatmari M, et al. Detection in life of confirmed Alzheimer's disease using a simple measurement of medial temporal lobe atrophy by computed tomography. *Lancet* 1993;340:1179–1183
15. de Leon MJ, McRae T, Tsai JR, et al. Abnormal hypercortisolemic response in Alzheimer's disease linked to hippocampal atrophy. *Lancet* 1988;ii:13:391–392
16. de Leon MJ, George AE, Stylopoulos LA, Smith G, Miller DC. Early marker for Alzheimer's disease: the atrophic hippocampus. *Lancet* 1989;ii:672–673
17. George AE, de Leon MJ, Stylopoulos LA, et al. CT diagnostic features of Alzheimer disease: importance of the choroidal/hippocampal fissure complex. *AJNR: Am J Neuroradiol* 1990;11:101–107
18. Duvernoy HM. *The human hippocampus: an atlas of applied anatomy*. Munich: JF Bergmann Verlag, 1988:16–145
19. Bobinski M, Morys J, Wegiel J, de Leon MJ, Miller DC, Wisniewski HM. Topography of pathological changes in the hippocampal formation in AD (abstr). *J Neuropathol Exp Neurol* 1992;51:318
20. de Leon MJ, Smith G, Convit A, et al. The early detection of brain pathology in Alzheimer's disease. In: Christen Y, Churchland P, eds. *Neurophilosophy and Alzheimer's disease*. New York: Springer-Verlag, 1992:131–143

20a. Convit A, de Leon MJ, Golomb J, et al. Hippocampal atrophy in early Alzheimer's disease: anatomic specificity and validation. *Psychiatr Quart* (in press)

21. Rosen WG, Terry RD, Fuld PA, Katzman R, Peck A. Pathological verification of ischemia score in differentiation of dementias. *Ann Neurol* 1980;7:486–488
22. Reisberg B, Ferris SH, de Leon MJ, Crook T. The global deterioration scale for assessment of primary degenerative dementia. *Am J Psychiatry* 1982;139:1136–1139
23. Gottlieb GL, Gur RE, Gur RC. Reliability of psychiatric scales in patients with dementia of the Alzheimer type. *Am J Psychiatry* 1988;45:857–859

24. Dura JR, Haywood-Niler E, Kiecolt-Glaser JK. Spousal caregivers of persons with Alzheimer's and Parkinson's disease dementia: a preliminary comparison. *Gerontologist* 1990;30:332–336
25. Reisberg B, Ferris SH, de Leon MJ, et al. Stage-specific behavioral, cognitive, and in vivo changes in community residing subjects with age-associated memory impairment (AAMI) and primary degenerative dementia of the Alzheimer type. *Drug Dev Res* 1988;15:101–114
26. American Psychiatric Association. *Diagnostic and statistical manual of mental disorders—revised.* 3rd ed. Washington: American Psychiatric Association, 1987:97–165
27. McKhann G, Drachman D, Folstein M, Katzman R, Price D, Stadlan EM. Clinical diagnosis of Alzheimer's disease: report of the NINCDS-ADRDA work group under the auspices of Department of Health & Human Services Task Force on Alzheimer's disease. *Neurology* 1984;34:939–944
28. Gilbert JG, Levee RF. Patterns of declining memory. *J Gerontol* 1971;26:70–75
29. Wechsler D. *Wechsler adult intelligence scale—Revised.* New York: Harcourt Brace Jovanovich, 1981:1–156
30. Folstein MF, Folstein SE, McHugh PR. Mini-mental state: a practical method for grading the cognitive state of patients for the clinician. *J Psychiatry Res* 1975;12:189–198
31. de Leon MJ, Ferris SH, George AE, Reisberg B, Kricheff II, Gershon S. Computed tomography evaluations of brain-behavior relationships in senile dementia of the Alzheimer's type. *Neurobiol Aging* 1980;1:60–69
32. de Leon MJ, George AE, Reisberg B, et al. Alzheimer's disease: longitudinal CT studies of ventricular change. *AJNR: Am J Neuroradiol* 1989;10:371–376
33. Berg L, Danziger WL, Storandt M, et al. Predictive features in mild senile dementia of the Alzheimer type. *Neurology* 1984;34:563–569
34. Flicker C, Ferris SH, Reisberg B. Mild cognitive impairment in the elderly: predictors of dementia. *Neurology* 1991;41:1006–1009
35. Ball MJ, Hachinski V, Fox A, et al. A new definition of Alzheimer's disease: a hippocampal dementia. *Lancet* 1985;5:14–16
36. Van Hoesen GW, Hyman BT, Damasio AR. Entorhinal cortex pathology in Alzheimer's disease. *Hippocampus* 1991;1:1–8
37. Miller AKH, Alston RL, Mountjoy CQ, Corsellis JAN. Automated differential cell counting on a sector of the normal human hippocampus: the influence of age. *Neuropathol Appl Neurobiol* 1984;10:123–141
38. Mann DMA, Esiri MM The site of the earliest lesions of Alzheimer's disease. *New Engl J Med* 1988;318:789–790
39. Gado M, Hughes CP, Danziger W, Chi D. Aging, dementia, and brain atrophy: a longitudinal computed tomographic study. *AJNR: Am J Neuroradiol* 1983;4:699–702
40. Brinkman SD, Largen J. Changes in brain ventricular size with repeated CAT scans in suspected Alzheimer's disease. *Am J Psychiatry* 1984;141:81–83
41. Luxenberg JS, Haxby JV, Creasey H, Sundaram M, Rapoport SI. Rate of ventricular enlargement in dementia of the Alzheimer type correlates with rate of neuropsychological deterioration. *Neurology* 1987;37:1135–1140
42. Golomb J, de Leon MJ, Kluger A, George AE, Tarshish C, Ferris SH. Hippocampal atrophy in normal aging: an association with recent memory impairment. *Arch Neurol* (in press)